Megawatt Infrared Laser Chemistry of $CHClF_2$. Photochemistry, Photophysics, and Molecular Dynamics of Excitation

Ernest Grunwald,* Kenneth J. Olszyna, David F. Dever, and Barry Knishkowy

Contribution from the Department of Chemistry, Brandeis University, Waltham, Massachusetts 02154. *Received February 7, 1977*

Abstract: Pulsed laser-irradiation of gaseous $CHClF_2$ at 1088 cm^{-1} causes decomposition to C_2F_4 and HCl, the same products as in homogeneous gas-phase thermolysis. Conversions per flash are as high as 50% with unfocused beams. Changing the surface/volume ratio or the irradiated fraction, in an attempt to change the cooling rate of the laser-heated gas, does not affect the conversion per flash (f). Relations between f and the absorbed energy per mole (E_{abs}), and between E_{abs} (or its equivalent, v_{abs}, the number of 1088 cm^{-1} einsteins absorbed per mole) and average dose ($\bar{D}$) are determined as functions of pressure, pulse duration, and added inert gas. For neat $CHClF_2$ in the pressure range 5.8–100 Torr, the photophysics is well described by $v_{abs}/\bar{D} = 1.50 + 30.64P/(P + 22.06)$ when $v_{abs} \gtrsim 2$. The same relation applies in the presence of an inert gas X, except that $P_{eff} = P + KP_X$ takes the place of P; $K = 0.21$ for He, 0.38 for N_2, and 0.7 for SiF_4. For neat $CHClF_2$, at pressures ranging from 1.6 to 100 Torr, v_{abs} ranging from 2 to 8.5, and pulse durations of 270 and 800 ns, the relation of f to E_{abs} is independent of pressure and pulse duration and is described in fair approximation by $f = A \exp(-E_{act}/E_{abs})$, where E_{act} is the known thermal activation energy of the primary process. Addition of inert gas reduces f below the value observed at the same E_{abs} in neat $CHClF_2$. The reduction can be formally described in terms of a spoil factor, s. For a given mole ratio of $CHClF_2$/X, s is independent of total pressure when X = SiF_4 and decreases with increasing pressure when X = He, so that there is no loss in photochemical efficiency as the total pressure is increased.

Molecular excitation by means of tunable infrared lasers is a convenient technique for initiating reactions of high activation energy.[2-7] The technique is especially efficient with pulsed lasers operating at infrared power levels of 0.1–10 MW/cm^2 and doses per flash of 0.03–0.5 J/cm^2.[6,7] We now report a quantitative study of the megawatt infrared laser chemistry of $CHClF_2$. The laser-induced reaction of this gas is particularly simple, being represented by

$$2CHClF_2 \rightarrow F_2C{=}CF_2 + 2HCl \qquad (1)$$

No products other than C_2F_4 and HCl were detected. These products are identical with those obtained in homogeneous gas-phase pyrolysis,[8] whose kinetics and thermochemistry are consistent with the following two-step mechanism:

$$HCClF_2 \underset{k_2}{\overset{k_1}{\rightleftharpoons}} CF_2 + HCl \qquad (2)$$

$$2CF_2 \xrightarrow{k_3} C_2F_4 \qquad (3)$$

Dissociation (rate constant k_1) is rate determining, with a limiting high-pressure activation energy of 234 kJ/mol.[8] As HCl accumulates, reaction of CF_2 with HCl (rate constant k_2) competes effectively with (3), and the net reaction rate decreases.[8] For the laser-induced reaction of $CHClF_2$, we find similarly that the amount of product per flash decreases as HCl accumulates. Thus, because of the identical products and the similar kinetic effect of HCl, we shall assume that the laser-induced reaction also proceeds by the two-step mechanism (2) and (3).

The infrared spectrum of gaseous $CHClF_2$ has been reported and all nine normal-mode frequencies have been assigned.[9] The very strong absorption band due to the antisymmetric CF_2 stretching vibration (ω_9 = 1114 cm^{-1}; symmetry A″)[9] has a P branch which falls into the tunable range of the CO_2 laser. We actually worked at 1088 cm^{-1} (line R36 of the 00°1–02°0 transition) where the output of our laser is quite uniform over a circular beam of 2 cm diameter. Absorbed-energy values as high as 125 kJ/mol and reaction per flash as high as 50% could be obtained with unfocused beams. Under our experimental conditions, molecules experience numerous collisions during the time of the laser flash so that the absorption of radiation is incoherent.

Definitions and Glossary of Symbols

I	intensity, in W/cm^2
D	dose/flash,[10] in J/cm^2; $D = \int I\,dt$
$\int$	denotes integration over one flash $I_D = \int I\,dD / \int dD = \int I^2\,dt / \int I\,dt$
τ	effective pulse duration (eq 4) $\tau = D/I_D = [\int I\,dt]^2 / \int I^2\,dt$ (4)
φ	irradiated fraction of gas; in a cylindrical cell, φ = (area of beam)/(inner cross-sectional area of cell)
CPF	fractional conversion of reactant to product, per flash, based on the full amount of gas in the irradiated cell; CPF = $(c_0 - c)/c_0$
CPF(%)	same as CPF, but expressed in percent
f	fractional conversion of reactant to product, per flash, based on the amount of gas actually irradiated by the laser beam; f = CPF/φ
f(%)	same as f, but expressed in percent
σ_D	fractional standard deviation of local dose measurements across the beam; see Figure 1
E_{abs}	radiant energy absorbed per mole of gas actually irradiated by the laser beam
v_{abs}	average number of infrared photons absorbed from the laser beam per molecule of the absorbing gaseous component; $v_{abs} = E_{abs}/N_0 h\nu$

Experimental Section

Materials. Gaseous $CHClF_2$ was obtained from Matheson Gas Products. The band maximum of the irradiated vibrational mode (ω_9) was at 1114 ± 1 cm^{-1}. The maxima of the first and second overtones were at 2217 ± 2 and 3307 ± 5 cm^{-1}, respectively. On the basis of these data, the anharmonic frequency shift for successive steps up the ω_9 vibrational ladder is −12 ± 2 cm^{-1}.

Nitrogen (Zero Gas) was obtained from Matheson, helium from Suburban Welders, and C_2F_4 from Peninsular Chemical Research, Inc. $CHClF_2$ and C_2F_4 were degassed and used without further pu-

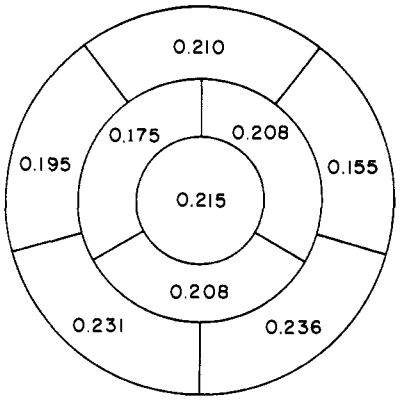

Figure 1. Typical results of local dose measurements across the laser beam.

rification. Standard manometric vacuum line techniques were used throughout.

Reaction Cells. In order that the irradiated fraction φ be close to unity and accurately known, most of the experiments were performed using a monel cell with interchangeable Teflon liners, which defined the optical path length. Optically flat, polished KCl windows, obtained from Janos Optical Co., were held against the Teflon liner by a metal sleeve and screw-on caps. O-rings between the metal sleeve and windows provided a vacuum-tight seal. The cross sectional area of the cell was 3.14 cm^2. A specially constructed hypodermic valve was used to minimize dead volume. The total dead volume was 0.014 cm^3.

The optical path length was adjusted so that 20–30% of the incident energy was absorbed. For reactant pressures of 100, 50, and 13.7 Torr, Teflon liners of 0.20, 0.40, and 2.6 cm, respectively, were inserted into the monel reaction cell. For reactant pressures of 5.6 and 1.6 Torr, cylindrical Pyrex cells, 9.5 and 47 cm in length, and with an inside diameter of 21 mm, were used. NaCl windows were mounted vacuum tight with glypt cement (6 C Electronics No. 90-2).

Laser. A Lumonics Model TEA 103 tunable pulsed CO_2 laser was used. Power profiles of the emitted radiation were measured with a Tachisto PD-1 photon drag detector, displayed on a Tektronix 7633 storage oscilloscope, and photographed. Two standard pulse profiles were used: (1) When the laser gas contains 4 vol % N_2, 83% of the dose is delivered in 300 ns, the remainder is delivered in the following 1100 ns; τ, calculated by numerical integration according to eq 4, is 270 ns. (2) When the laser gas contains 10 vol % N_2, 44% of the dose is delivered in 300 ns, the remainder is delivered in the following 3000 ns; τ = 800 ns.

The laser beam, of 1 cm radius, was adjusted to optimum homogeneity, as indicated by burn patterns. The dose distribution across the beam was monitored by the following method: The beam area was divided into nine equal segments, as shown in Figure 1. Using a plastic mask with an 0.089-cm^2 hole mounted on a precision-ruled vertical- and cross-feed carrier, the dose was measured at the center of each segment. A typical result is indicated in Figure 1. The standard deviation of the local dose measurements, expressed as percent of the mean of the local dose measurements, ranged from 6 to 18%. Coherence of the radiation across the laser beam was evident from Fresnel diffraction rings whenever the beam was truncated by means of a circular aperture. From the manufacturers specification for bandwidth, the coherence time of the radiation was estimated to be ~0.5 ns.

Dosimetry. Special attention was paid to accuracy, because a 10% error in E_{abs} corresponds to a 30–60% error in f. A diagram of the optical arrangement is shown in Figure 2. The laser beam passes through a diverging germanium lens L, of focal length 1.33 m, which permits convenient attenuation of the dose. At a suitable distance from L, the laser beam is truncated by a circular opening of 0.87-cm radius in a plastic mask M. About 14% of the transmitted radiation is deflected by a beam splitter BS onto detector M1. The remainder passes through the cell and is detected by M2. If necessary, a flat CaF_2 attenuator A is inserted between the cell and M2 to avoid overloading of M2.

M1 is a pyroelectric detector whose voltage output is observed on a storage oscilloscope. M1 is used only to monitor small changes from pulse to pulse in the laser output. The primary detector is M2, a

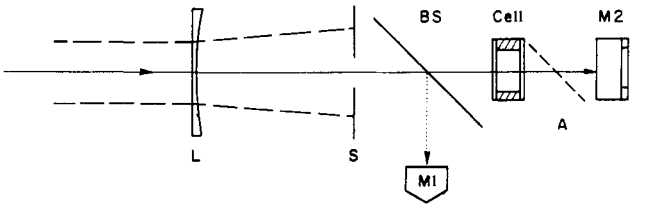

Figure 2. Schematic diagram of components on optical bench: L = lens; S = plastic mask; BS = germanium beam splitter; A = CaF_2 attenuator; M1 = pyroelectric detector; M2 = disk calorimeter.

Scientech disk calorimeter.[11] An "experiment" consists of measurements of radiant energy with (a) the cell removed from, (b) an evacuated cell in, and (c) a gas-filled cell in, the optical path. In the disk calorimeter, 98–99% of the radiant energy (a figure which we have confirmed) is absorbed by a thin disk whose temperature rise, and eventual return to ambient temperature owing to thermal conduction to a heat sink, are monitored by means of a thermopile. To permit direct calibration in terms of electrical energy, the reverse side of the radiation-absorbing disk is in intimate contact with a 40-ohm heating wire through which the electric charge stored by a capacitor may be discharged. We found that, when the RC time constant of this electrical circuit is >0.5 ms, 99–100% of the electrical energy ($\frac{1}{2}CV^2$) is transferred to the disk, producing a temperature rise and eventual return to ambient temperature simulating the thermal effect of a pulse of absorbed radiation. The energy absorbed by the disk in either case is proportional to $\int e\,dt$, where e is the thermal emf of the thermopile and the integration is over the entire thermal cycle triggered by the absorption of either radiant or electrical energy. To obtain the value of $\frac{1}{2}CV^2$ required for electrical calibration, the capacitance C was measured with a General Radio Type 1680 A system; high-quality nonelectrolytic capacitors totaling 22.14 μF were used. The dc voltage V was measured with a Hewlett-Packard 3465 A $4\frac{1}{2}$ digit multimeter and ranged from 100 to 300 V.

To obtain $\int e\,dt$, the thermal emf was amplified from ~1, to ~600 mV, digitized, transferred to a programmable calculator, and integrated numerically. Return of the thermal emf to ambient (zero) was a first-order process with half-life of 7.2 s. After 12.5 s, integration to $t = \infty$ was done analytically, by applying a first-order rate law. Results for the calibration factor, $\int e\,dt/(\frac{1}{2}CV^2)$, were precise with standard deviation of ~1% over a two to three fold change of $\frac{1}{2}CV^2$. Results for (radiant dose)/(reference meter M1 reading) eventually became precise to 2%.

Analytical Techniques. Optical components were aligned carefully on an optical bench so that the infrared beam passed precisely through the geometrical center of the reaction cell. The position of the infrared beam was checked with burn patterns to make sure it did not hit the cell wall. The beam area was calculated at the center of the cell and in no case changed by more than 3.3% from the front to the back of the cell.

Average dose in the cell ($\bar{D}$) and E_{abs} were calculated as follows. Let D_{air}, D_{MT}, and D_{gas} denote the dose (in J/cm^2) measured by M2 when the beam passes through air, the empty cell, and the gas-filled cell, respectively. Let L denote the cell length, $\mathbf{t}$ the optical transmission coefficient at the interface between air and KCl or NaCl, $r = 1 - \mathbf{t}$, and let α denote the dose attenuation by the gas in the cell in one pass of the beam. Setting $1 - r^2 \doteq 1$ throughout, we obtain

$$D_{MT}/D_{air} = \mathbf{t}^4/(1 - r^2)^3 \doteq \mathbf{t}^4 \quad (5)$$

$$D_{gas}/D_{MT} = \alpha \quad (6)$$

$$\bar{D} = \tfrac{1}{2}D_{air}\mathbf{t}^2(1 + [1 + r + r\mathbf{t}^2]\alpha + [r + r\mathbf{t}^2]\alpha^2) \quad (7)$$

$$D_{abs} = D_{air}\mathbf{t}^2(1 - \alpha)(1 + [r + r\mathbf{t}^2]\alpha) \quad (8)$$

$$E_{abs} = D_{abs}RT/PL \quad \text{(J/mol)} \quad (9)$$

Values of $\mathbf{t}$ based on the refractive index at 1088 cm^{-1} (0.960 for NaCl and 0.965 for KCl) were in reasonable agreement (~0.5%) with experimental values; the latter were usually smaller. For the reflected radiation, the theoretical value ($1 - \mathbf{t}^4$) is 13.3% for KCl; the experimental value was 14 ± 1%. Typical values of α were 0.7–0.8. The experimental accuracy of $\bar{D}$ improved during this work, being about 3% for most measurements. The corresponding error in E_{abs} is 10–15%.

Table I. Effect of Cooling Rate on Amount of Reaction per Flash for $CHClF_2$[a]

P, Torr	E_{abs}, kJ/mol	Cell size L × R, cm	φ	f(obsd), %	Calcd f(%), T-jump model C + R	Calcd f(%), T-jump model C + R + M
14.2	32.0[c]	2.6 × 1.0	0.895	0.173	(0.173)[b]	(0.173)[b]
		0.4 × 1.0	0.895	0.22	0.044	0.018
13.0	75.5	2.6 × 1.0	0.777	15.2	(15.2)[b]	(15.2)[b]
		0.4 × 1.0	0.777	15.5	4.5	1.7
29.5	110.7	0.8 × 1.0	0.777	49.8	(49.8)[b]	(49.8)[b]
		0.4 × 1.0	0.777	45.2	37.1	20.6
50	100[d]	0.4 × 1.6	0.721	37.4		(37.4)[b]
		0.4 × 1.6	0.300	34.3		7×10^{-5}

[a] Infrared pulse duration is 270 ns throughout. $\bar{\nu} = 1088\ cm^{-1}$, except where indicated. [b] Magnitude of T-jump adjusted to give agreement with experiment for the longer cell. C + R, cooling by conduction and radiation; C + R + M, conductive and radiative cooling accompanied by perfect mixing. See text for details. [c] $\bar{\nu} = 1087\ cm^{-1}$; $v_{abs}/\bar{D} = 10.6$. [d] Measured with pyroelectric meter; less accurate.

Amount of reaction was monitored by observing the disappearance of the reactant and the appearance of C_2F_4 by before and after infrared scans between 2000 and 600 cm^{-1}, using a Perkin-Elmer Model 567 spectrophotometer. Except in single-flash experiments, the number of flashes was adjusted so that 5–15% of the reactant disappeared. Because of the small change of the concentration of the reactant, the accuracy of the CPF is only about 15%; the amount of C_2F_4 produced generally agreed within this limit. It did not seem worthwhile to improve the accuracy beyond this figure because a 10% change in E_{abs}, which is still within the experimental error in E_{abs}, would produce a ~40% change in f.

Most of the results listed in the tables are averages based on two or more independent experiments. This is especially true of results in which f is determined as a function of cell length or pulse duration at constant E_{abs}. In such comparisons, deviations of E_{abs} from exact equality should be no greater than 10%.

Effect of Beam Inhomogeneity. We now establish functional relationships between D, E_{abs}, and f. However, owing to the inhomogeneity of the dose across the laser beam, and to absorption along the optical path in the cell, we are actually working with averages. Thus, for any two variables y and x, the function we actually obtain is *not* $y = F(x)$, but $\bar{y} = G(\bar{x})$, where $\bar{y}$ and $\bar{x}$ are mean values. The functions $G(\bar{x})$ and $F(x)$ are not rigorously the same. To derive the relationship, we expand $y_i = F(x_i)$ about the mean $\bar{x}$ and obtain

$$y_i = F(\bar{x}) + F'(\bar{x})(x_i - \bar{x}) + F''(\bar{x})(x_i - \bar{x})^2/2 + \ldots \quad (10)$$

On calculating the mean $\bar{y}$ from (10), we then find that $\bar{y}$ is the sum of $F(\bar{x})$ and of higher-order terms which contain as factors the successive derivatives of $F(x)$ and successive moments about the mean of the distribution of x:

$$\bar{y} = F(\bar{x}) + F''(\bar{x})\sigma_x^2/2 + \ldots \quad (11)$$

The derivation of (11) from (10) becomes obvious when we recall that the first moment about the mean is zero and the second moment is σ_x^2, where σ denotes the standard deviation from the mean. Equation 11 leads at once to the desired relationship:

$$G(\bar{x}) = F(\bar{x}) + F''(\bar{x})\sigma_x^2/2 + \ldots \quad (12)$$

According to (12), when y is a linear function of x, $\bar{y} = F(\bar{x})$, regardless of how inhomogeneous the distribution might be. For slightly curved relationships $G(\bar{x})$ and $F(\bar{x})$ still remain essentially equal, especially if the inhomogeneity of x is fairly small. Thus the observed relationships between E_{abs} and the average dose $\bar{D}$ (see below) are essentially independent of beam inhomogeneity, a conclusion which we have verified experimentally. On the other hand, relationships between f and E_{abs} turn out to be highly curved, and corrections for beam inhomogeneity will be significant.

A six-page Appendix dealing with calculations of *cooling dynamics* and *inhomogeneity of laser dose* may be obtained from the authors upon request.

Results

Effect of Cell Geometry and Beam Size. In an attempt to determine whether the laser-induced reaction proceeds by a thermal mechanism, experiments were performed in which the surface/volume ratio and fraction φ of the irradiated gas were varied. Other variables, such as E_{abs}, pulse duration, gas pressure, and composition, were kept constant. If reaction were proceeding by a thermal mechanism, one would expect a smaller conversion per flash in the experiments with the greater surface/volume ratio or the smaller irradiated fraction, in which the laser-heated gas would be expected to cool more quickly.

Results, which cover a representative range of pressure and E_{abs}, are listed in Table I. Because in comparable experiments, deviations of E_{abs} from exact equality owing to experimental error may be as high as 10%, differences in f of <40% are not statistically significant. Actual differences in f, on increasing the cell length or beam size, range from −26 to +10%, with a mean absolute value of 12%. Clearly, within the experimental error, the amount of reaction per flash is unaffected by the cooling dynamics.

Predictions for Thermal Reaction. To complete the analysis we must show that a model of sudden temperature jump followed by cooling with normal thermal reaction would have given detectable differences in f. Rate constants for the thermal reaction of $CHClF_2$ have been reported[8] and are reproduced by the empirical equation, $\log k = 12.6 - 11540/T$.

To predict local temperature vs. time profiles in the reaction cell, we shall use two models which represent opposite extremes in the treatment of mass flow during cooling, and which are capable of explicit mathematical solution. In each model one calculates f as a function of an initial gas temperature T_M, the temperature reached when the absorbed energy E_{abs} (assumed to be constant throughout the irradiated volume) produces a sudden temperature jump. In the model denoted by C + R, cooling takes place by conduction[12] and radiation[13] only; mass flow is neglected. In the model denoted by C + R + M, mixing of volume elements, following each infinitesimal step of cooling by conduction and radiation, is so efficient that the gas effectively cools at uniform pressure and temperature. Mathematical details are available from the author (see above). Briefly, local values of $\int k\ dt$ lead to local values of f, which are then averaged by numerical integration over the entire cell.

In presenting the model predictions in Table I, T_M is adjusted so that the model gives perfect agreement with experiment for f in the longer cell. The same value of T_M is then used to predict a consistent value of f for the shorter cell. With one exception, the predicted changes in f exceed factors of 2 and would have been detected easily. Since our experiments show no such changes, and indeed show no significant changes at all, we must conclude that reaction takes place *before* rather than after the absorbed energy has become random thermal energy.

E_{abs} as a Function of Dose. It is convenient to divide the

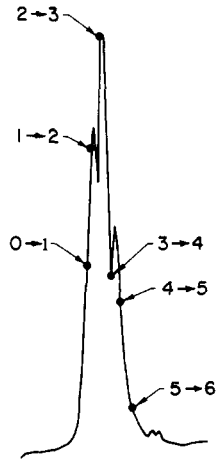

Figure 3. Band envelope of the irradiated ω_9 mode of $CHClF_2$, showing the progressive changes of the rotational factor in the transition probability as the molecules step up the vibrational ladder by absorbing 1088-cm^{-1} photons.

overall problem of infrared laser chemistry into (a) absorption of energy, and (b) amount of reaction as a function of E_{abs}. For $CHClF_2$, the phenomenology of energy absorption in our experimental range is similar to, but simpler than, that reported recently for SiF_4.[14] For comparison with properties of the energy-absorbing molecular oscillators, it is convenient to express E_{abs} as a multiple of the energy per mole of 1088-cm^{-1} photons.

$$E_{abs} = \upsilon_{abs} N_0 h\nu \qquad (13)$$

υ_{abs} is the *mean excitation number* of the oscillators, and $N_0 h\nu$ = 13.02 kJ/einstein at 1088 cm^{-1}.

Neat $CHClF_2$. Data for neat $CHClF_2$ at pressures ranging from 100 to 1.6 Torr and υ_{abs} ranging from 1.2 to 8 are listed in Table II. The data show that *at constant pressure*, when $\upsilon_{abs} > 2$, υ_{abs} is simply proportional to $\overline{D}$, the values of $\upsilon_{abs}/\overline{D}$ being constant within the 10% experimental error. As υ_{abs} becomes < 2, $\upsilon_{abs}/\overline{D}$ appears to decrease.

The average slopes ($\upsilon_{abs}/\overline{D}$) obtained at constant pressure in the proportional range increase with the pressure. The increase is nonlinear and the function tends toward a high-pressure limit. The data are represented satisfactorily by a three-parameter equation of the form

$$\upsilon_{abs}/\overline{D} = AP/(P + B) + C \qquad (14)$$

The equation contains a small additive constant, C, because energy absorption does not tend toward zero at $P \rightarrow 0$ but approaches an unknown but finite value characteristic of the coherent mechanism. The success of (14) at reproducing the data at 1088 cm^{-1} with A = 30.64, B = 22.06, and C = 1.50 is indicated in the final column of Table II.

According to (14), for $CHClF_2$ at 1088 cm^{-1}, absorption of megawatt infrared radiation is actually more efficient, at sufficiently high pressures, than of low intensity radiation. The high-pressure limit of $\upsilon_{abs}/\overline{D}$ according to (14) is 32.1 J^{-1} cm^2, while at low intensities $\upsilon_{abs}/\overline{D}$ is calculated to be ~20 J^{-1} cm^2 from the spectrophotometric percent transmission.

Although it must be stressed that eq 14 is an empirical relationship whose range of validity has not been fully established, we note that exact proportionality between υ_{abs} and D is characteristic of resonant absorption by an ensemble of harmonic oscillators. In order to probe the observed proportionality existing at $\upsilon_{abs} > 2$, we show in Figure 3 the band envelope of the irradiated ω_9 mode, whose shape results largely from rotational coupling. Owing to the anharmonic frequency shift of 12 cm^{-1}, the rotational factor in the transition probability moves progressively to the right as the molecules step up the vibrational ladder while absorbing 1088-cm^{-1} photons. As shown in Figure 3, the rotational factor is therefore expected to increase up to $\upsilon = 3$ and then to decrease progressively and markedly, become quite small above $\upsilon = 6$. By contrast, the data in Table II show no evidence for a reduction in transition probability with increasing υ_{abs} up to the highest value, υ_{abs} = 8.5.

Table II. Neat $CHClF_2$ Irradiated at 1088 cm^{-1} [a]

P, Torr	σ_{beam}, %	υ_{abs}	$\upsilon_{abs}/\overline{D}$, J^{-1} cm^2	f, %	$\upsilon_{abs}/\overline{D}$ (calcd)[b]
		τ = 270 ns			
100	16	6.67	26.9	31	26.6
	10	5.84	27.8	24.5	
	13	4.91	27.5	11.9	
	12	4.86	29.2	6.5	
	16	3.13	24.3	0.84	
	16	2.75	25.9	0.15	
	16	1.77	20.1	0.021	
50	18	5.11	22.6	15.7	22.8
	18	4.01	22.5	3.0	
	21	3.14	21.2	0.59	
	30	2.00	18.0	0.030	
		1.17	14.7		
29.5	12	8.51	20.0	49.8	19.0
13.0	17	5.25	13.4	12.9	13.2
13.7	40	4.87	13.6	11.3	
	13	3.66	12.8	1.27	
	16	2.71	11.9	0.14	
	14	1.75	12.1	~0.011	
5.8	~10	3.41	8.3	0.68	7.9
5.6		1.46	7.3		
1.56	16	1.27	3.1		3.5
		τ = 800 ns; increase in $\upsilon_{abs}/\overline{D}$			
50	18	3.81	24.2	2.6	+8%[c]
1.59	12	4.04	6.2	1.04	+100%[c]

[a] φ is 0.8–0.9, α is 0.7–0.8 throughout. [b] $\upsilon_{abs}/\overline{D} = 1.50 + 30.64P/(P + 22.06)$. [c] Percent increase in $\upsilon_{abs}/\overline{D}$ at 800-ns pulse duration relative to 270-ns pulse duration.

That $\upsilon_{abs}/\overline{D}$ for incoherent excitation at high intensities should fall off with decreasing pressure is both expected and normal. The reason for this is that the optical transition will become saturated unless the populations of the rotational levels that are brought into resonance by the laser frequency remain in equilibrium with the rotational-level populations at large. However, the mathematical form of eq 14 is surprising because the empirical factor $P/(P + B)$ depends only on the pressure and not on the intensity.

If $\upsilon_{abs}/\overline{D}$ is really independent of intensity, then one expects that at constant pressure it is also independent of the pulse duration τ. Our meager data are listed at the end of Table II and in note *d* of Table III. At 50 Torr of $CHClF_2$ the effect of increasing τ from 270 to 800 ns is indeed insignificant, being +8% for the neat gas and −9% in the presence of nitrogen. At 1.6 Torr the change of +100% is statistically highly significant, but the interpretation is a little uncertain because at least part of the increase may be due to the fact that υ_{abs} for the shorter pulse is only 1.3, well below the usual starting point of the proportional range.

Effect of Inert Gases. Our data for υ_{abs} as a function of dose in the presence of inert gases are listed in Table III. In general, the added gas pressure increases the value of υ_{abs}/D, with an efficiency depending on the nature of the added molecules. Because all the data in Table III lie in the range of excitation numbers where eq 14 would apply for the neat gas, we have tried the following generalized version:

Table III. $CHClF_2$ Irradiated in the Presence of Inert Gases at 1088 cm^{-1} (τ = 270 ns)

P_{CHClF_2}, Torr	P_X Torr	v_{abs}	$v_{abs}/\bar{D}$, J^{-1} cm^2	f, %	$v_{abs}/\bar{D}$ (calcd)[a]	*quasi*-v_{abs}[b]	Spoil factor[c]
			X = helium; K = 0.21				
5.8	11.6	3.92	10.3		9.8		
	11.6	4.41	10.9	0.14	9.8	2.52	0.38
	29.0	4.32	12.8		12.2		
	29.0	5.29	13.0	0.042	12.2	2.05	0.32
	116	5.86	17.2		19.2		
	116	6.38	17.6	~0.0011	19.2		
50	250	4.76	26.4	0.13	26.7	2.49	0.18
			X = nitrogen; K = 0.38				
5.8	5.8	3.95	10.6	0.092	9.7	2.29	0.72
	11.6	4.21	10.9	0.031	11.2	1.95	0.58
	29.0	4.87	14.1		14.7		
50	250	7.26	31.7[d]	0.11	28.1	2.38	0.41
			X = SiF_4; K = 0.7				
8.6	3.89	4.86	11.6	0.51	11.9	3.04	1.33
50	23	5.73	27.0	0.95	24.5	3.34	1.55
	23	9.10	23.6	26.4	24.5	6.06	1.09

[a] $v_{abs}/\bar{D} = 1.50 + 30.64P_{eff}/(P_{eff} + 22.06)$; $P_{eff} = P_{CHClF_2} + KP_X$. [b] Value of v_{abs} at which neat $CHClF_2$ would give the same f as is observed for the mixture. [c] *quasi*-$v_{abs}/v_{abs} = P_{CHClF_2}/(P_{CHClF_2} + sP_X)$; s = spoil factor. [d] When τ = 800 ns, $v_{abs}/\bar{D}$ = 28.9.

Table IV. Effect of Pulse Duration on Yield per Flash for $CHClF_2$ at 1088 cm^{-1}

P, Torr	v_{abs}	τ, ns	f, %	$\delta f/f$ × 10^2	Z_τ[a]
50/$CHClF_2$	3.81	270	2.1		177
		800	2.6	+24	524
9.4/$CHClF_2$	3.78[b]	270	1.6		33
		800	1.7	+6	99
9.4/$CHClF_2$	5.16[b]	270	11.6		33
		800	8.8	−24	99
50/$CHClF_2$	7.26	270	0.11		850
+ 250/N_2		800	0.11	0	2500

[a] $Z_\tau = 1.31 \times 10^7 P\tau$, where P is in Torr and τ in seconds. See ref 16. [b] Measured with a pyroelectric energy meter. Absolute value of v_{abs} is less accurate, but comparison of f at two values of τ is as precise as in experiments with a disk calorimeter.

$$v_{abs}/\bar{D} = AP_{eff}/(P_{eff} + B) + C \quad (15)$$

where the parameters A, B, and C have the same values as before, and P_{eff} is an *effective* pressure defined in

$$P_{eff} = P_{CHClF_2} + KP_X \quad (16)$$

K is a constant characteristic of the added gas which measures the relative efficiency of collisions between $CHClF_2$ and added-gas molecules at raising $v_{abs}/\bar{D}$ for $CHClF_2$.

Suitable values of K and correspondingly calculated values of $v_{abs}/\bar{D}$ for each added gas are included in Table III. On the whole, the treatment is successful in reproducing the data to a good first approximation. Moreover, the values of K vary in a rational manner, increasing monotonically with the molecular weight of X and hence with the reduced mass $m_X m_{CHClF_2}/(m_X + m_{CHClF_2})$ of the bimolecular collision complex. Efficiency per collision may be expected to increase with reduced mass when the amount of energy to be transferred is small.[15]

Yield per Flash as a Function of v_{abs}. We shall examine the relation of f vs. v_{abs} as a function of effective pulse duration, pressure, and added inert gas.

Effect of Pulse Duration. Data for f vs. τ at otherwise constant conditions are listed in Table IV for a threefold change in τ and representative values of P and v_{abs}. As in previous comparisons, differences in f of <40% are not statistically

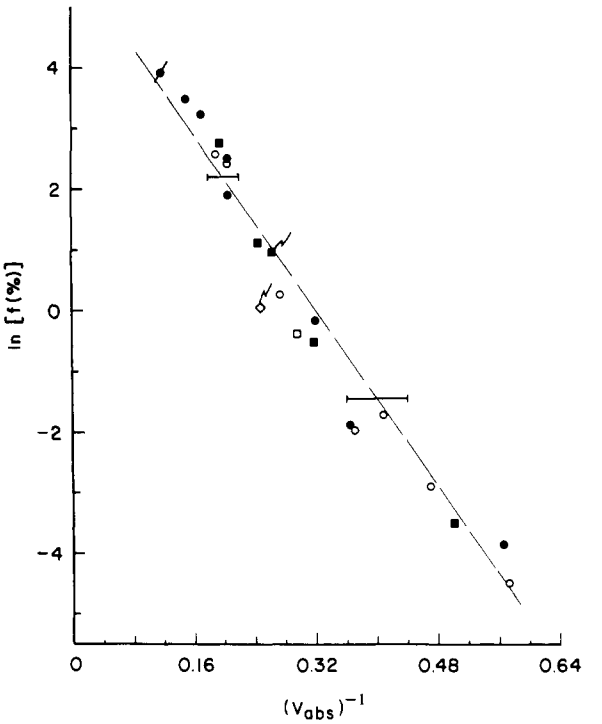

Figure 4. Photochemical results for neat $CHClF_2$ as a function of pressure: (●) 100 Torr, (■) 50 Torr, (◆) 29.5 Torr, (○) 14.2, 13.7, 13.0 Torr, (□) 5.8 Torr, (◇) 1.6 Torr. Points marked by a flagellum, τ = 800 ns; others, τ = 270 ns. The dashed line is drawn with a slope equivalent to E_{act} = 234 kJ/mol.

significant. Bearing this in mind, f is independent of τ, with a high statistical probability, under all conditions.

Table IV also lists values of Z_τ, the mean number of gas-kinetic collisions experienced by a molecule of $CHClF_2$ during the time τ. For neat $CHClF_2$, these values range from 33 to 524 and bracket the value of Z_{10}, 268 collisions, required for V-T/R relaxation of $CHClF_2$.[16]

Effect of Pressure. Results for f vs. v_{abs} for neat $CHClF_2$ are listed in Tables I and II. A plot of these results, which includes pressures ranging from 100 to 1.6 Torr, is shown in Figure 4. Between 100 and 5.8 Torr, all experimental points clearly define a single, pressure-independent relationship. The deviation from this relationship at 1.6 Torr is only marginally

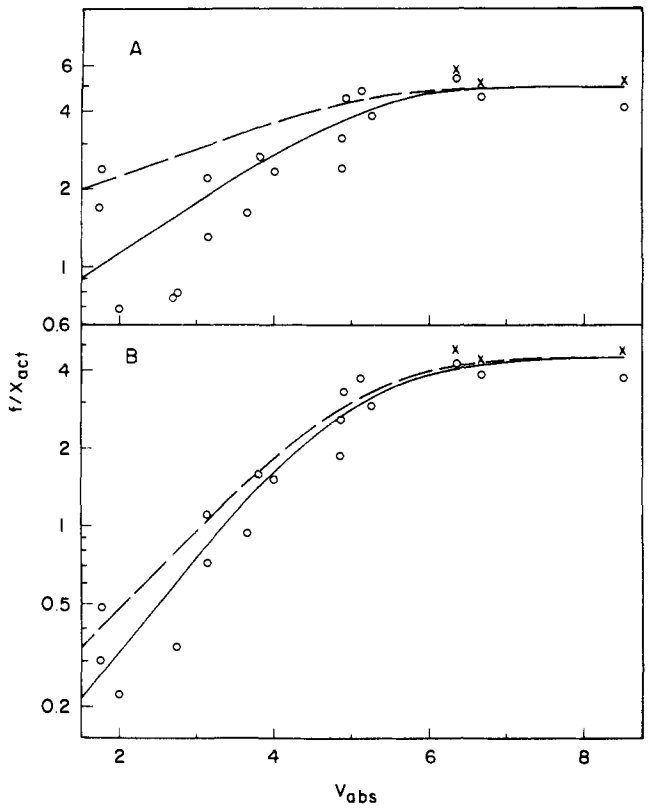

Figure 5. Plot of f/x_{act} vs. v_{abs}: (A) eq 19; (B) eq 20: dashed lines, uncorrected; solid lines, corrected for beam inhomogeneity; circles, inhomogeneity-corrected experimental points; crosses, see footnote 18.

significant. Thus, both variations of τ and of pressure show consistently that the relationship between f and E_{abs} is independent of the number of collisions which the absorbing molecules experience during the time of the laser pulse. In the 100 to 5.8 Torr experiments plotted in Figure 4, Z_τ ranges from 500 to 20 collisions.

Exponential Dependence on E_{abs}^{-1}. It has been shown, in publications from this[6] and other[17] laboratories, that the variation of f with E_{abs} at values of v_{abs} and P similar to ours conforms rather well to

$$f = A \exp(-E_{act}/E_{abs}) \qquad (17)$$

where A is a parameter and E_{act} is the thermal activation energy of the laser-induced primary decomposition step. In the present case E_{act} = 234 kJ/mol[8] (v_{act} = 18.0). Accordingly, the dashed line in Figure 4 represents the relationship, $f(\%)$ = constant × $\exp(-18.0/v_{abs})$, which clearly gives a respectable fit.

Effect of Added Gases. Table III includes our data for f as a function of v_{abs} in the presence of inert gases. As a general rule, the presence of inert gas depresses the amount of reaction. To quantify this effect, we defined a function *quasi-*v_{abs}, which is simply the value that v_{abs} would assume if the same value of f had been observed in the absence of the added gas. Values of *quasi-*v_{abs} were obtained by interpolation from Figure 4 and are listed in column 7 of Table III. They are considerably smaller than the real values of v_{abs}, which are listed in column 3, showing that some of the absorbed energy has been "spoiled" for effective use. To obtain a measure of this effect, we introduce the *spoil factor*, s, for the inert gas according to

$$quasi\text{-}v_{abs}/v_{abs} = P_{CHClF_2}/(P_{CHClF_2} + sP_X) \qquad (18)$$

Because of the ad hoc manner of its definition, s need not be a constant factor but may vary with the experimental conditions. However, having found that the relationship between f and E_{abs} for neat $CHClF_2$ is independent of the pressure, we now hope that the "spoiling" of excitation energy by the added gas depends on the pressure ratio, P_X/P_{CHClF_2}, rather than on the absolute value of P_X. Hence the right side of (18) has been written in the form of a kinetic partition factor.

In Table III, the pressure ratios range from 2 to 20 for He, from 1 to 5 for N_2; and it is 0.46 for SiF_4. $CHClF_2$ pressures range from 5.8 to 50 Torr. Within the limited scope of these data it appears that at constant pressure ratio, s is either independent of total pressure (data for SiF_4), or *decreases* with increasing pressure (data for He). At constant P_{CHClF_2}, for both He and N_2, s *decreases* with increasing pressure ratio. Since s measures the spoiling efficiency per Torr of added gas, a decrease of s indicates a *smaller deleterious effect* per Torr. Thus the data encourage the hope that when the added gas is a potential reactant, laser-induced bimolecular reactions will be both possible and probable, at conveniently high pressures, and even under conditions where the infrared-absorbing species is relatively dilute.

Discussion

Three conclusions seem to emerge from our results. (1) The laser-induced decomposition of $CHClF_2$ under the present conditions does not proceed by a thermal mechanism. (2) The amount of energy absorbed from a given dose increases with the pressure ("effective pressure" in the case of gas mixtures) and approaches asymptotically to a high-pressure limit. (3) For a given amount of absorbed energy, the amount of reaction per flash is independent of the number of collisions during the flash.

Because of (1), we shall assume that decomposition takes place within a relatively short time after completion of the laser flash. Therefore the amount of reaction will be a sensitive function of the molecular energy distribution existing at the end of the laser flash. Because of this, we infer from (3) that the molecular energy distribution is not altered by collisions during the laser flash. Because the energy is being absorbed in quanta of $h\nu$, the radiation field then constrains the excitation energies of the molecules to integral multiples of $h\nu$. That is, the levels of excitation are equidistant, just like those of a harmonic oscillator.

In previous publications from this laboratory[6,7] the working hypothesis was made that the molecular energy distribution among the equidistant levels of excitation is a Boltzmann distribution for a single harmonic oscillator. On that basis, the relationship between f and E_{abs} could reasonably be expressed by eq 17, in agreement with available data. We now wish to probe this matter further, by comparing actual amounts of reaction per flash, f, with predicted fractions x_{act} of molecules which have an excitation energy equal to, or greater than, the required activation energy at the end of the laser pulse. If x_{act} is predicted correctly, f/x_{act} becomes formally analogous to the quantum yield Φ in conventional photochemical reactions.

If the absorbed energy is constrained to a single harmonic set of levels according to a Boltzmann distribution, then x_{act} at the end of the laser pulse will be given approximately by

$$x_{act} = \exp(-E_{act}/E_{abs}) = \exp(-v_{act}/v_{abs}) \qquad (19)$$

and exactly by

$$x_{act} = [v_{abs}/(1 + v_{abs})]^{v_{act}} \qquad (20)$$

Plots of f/x_{act} vs. v_{abs} based on these equations are shown in Figures 5A and 5B, respectively. The solid curves in both figures represent the experimental data when x_{act} is calculated so as to take beam inhomogeneity into account. (See Experimental Section (eq 11) and additional material available from author.) The dashed curves represent the experimental data

without correction for beam inhomogeneity; that is, to the same level of approximation as in Figure 4.

Three observations are worth making. (1) In the quantitative interpretation of data, beam inhomogeneity needs to be taken into account, especially at low dosages. (2) The empirical eq 17 is not an exact relationship, because neither of the curves in Figure 5A is a horizontal straight line. According to the dashed curve, the parameter A in (17) varies by a factor of ~2 while $\exp(-v_{act}/v_{abs})$ varies by a factor of ~3000. (3) All relationships shown in Figure 5 increase up to $v_{act} \sim 5$ and appear to become constant when $v_{act} > 5$.[18] This feature is shown most clearly by the solid curve in Figure 5B, which is based on the exact harmonic oscillator, eq 20. The maximum value of f/x_{act} is about 5, which means that the amount of laser-induced reaction is greater than the fraction of activated molecules predicted by the simple harmonic oscillator model.

References and Notes

(1) Work supported by the National Science Foundation.
(2) (a) M. W. Berry, *Annu. Rev. Phys. Chem.*, **26**, 263–268 (1975); (b) J. T. Knudtson and E. M. Eyring, *ibid.*, **25**, 255 (1974).
(3) W. M. Shaub and S. H. Bauer, *Int. J. Chem. Kinet.*, **7**, 509 (1975).
(4) N. V. Karlov, *Appl. Opt.*, **13**, 301 (1974).
(5) I. Glatt and A. Yogev, *J. Am. Chem. Soc.*, **98**, 7087 (1976).
(6) D. F. Dever and E. Grunwald, *J. Am. Chem. Soc.*, **98**, 5055 (1976).
(7) E. Grunwald and K. J. Olszyna, *Laser Focus*, **12**(6), 41 (1976).
(8) R. G. Barnes, R. A. Cox, and R. F. Simmons, *J. Chem. Soc. B*, 1176 (1971).
(9) E. K. Plyler and W. S. Benedict, *J. Res. Natl. Bur. Stand.*, **47**, 212 (1951).
(10) Synonymous with dose/flash are the terms "energy flux" or "energy fluence". We prefer to retain the traditional term "dose", which has been used for many years in such fields as X-radiology and radiation chemistry.
(11) (a) E. D. West and D. A. Jennings, *Rev. Sci. Instrum.*, **41**, 565 (1970); (b) R. W. Zimmerer, "Theory and Practice of Thermoelectric Laser Power and Energy Measurement", Scientech Inc., Boulder, Colo., May 1976.
(12) A. V. Lykov, "Analytical Heat Diffusion Theory", J. P. Hartnett, Ed., Academic Press, New York, N.Y., 1968.
(13) M. Jakob, *Proc. Phys. Soc. London*, **59**, 728 (1947).
(14) K. J. Olszyna, E. Grunwald, P. M. Keehn, and S. P. Anderson, *Tetrahedron Lett.*, 1609 (1977).
(15) R. N. Schwartz, Z. I. Slawsky, and K. F. Herzfeld, *J. Chem. Phys.*, **20**, 1591 (1952).
(16) T. D. Rossing and S. Legvold, *J. Chem. Phys.*, **23**, 1118 (1955).
(17) J. M. Preses, R. E. Weston, Jr., and G. W. Flynn, *Chem. Phys. Lett.*, **46**, 69 (1977).
(18) Because f/x_{act} approaches unity in the limit as v_{act} becomes large, the crosses in Figure 5 represent the function $\ln(1-f)/\ln(1-x_{act})$, which does not approach any mathematically required limit as v_{act} becomes large. $\ln(1-f)/\ln(1-x_{act})$ practically reduces to f/x_{act} except in the three experiments in which $v_{act} > 6$. The use of $\ln(1-f) = -\ln(c_0/c)$ in place of f seems logical for expressing amount of reaction in an inquiry which probes the chemical kinetics.

Megawatt Infrared Laser Chemistry of CCl_2F_2 Derived from the Excitation of Two Distinct Vibrational Modes[1]

Gregory A. Hill, Ernest Grunwald,* and Philip Keehn

Contribution from the Department of Chemistry, Brandeis University, Waltham, Massachusetts 02154.

Received February 25, 1977

Abstract: CCl_2F_2 was pulse irradiated at 921 cm^{-1}, where a CCl_2 stretching mode is excited, and at 1088 cm^{-1}, where a CF_2 stretching mode is excited. Laser-induced reactions at the two frequencies are practically identical, both qualitatively and quantitatively. Major reaction products are ClF_2CCClF_2 and $CClF_3$ and account for ~83% of decomposition. Minor products formed initially are ClF_2CCCl_2F and CCl_3F; there was no evidence for C_2F_4. A reaction mechanism involving primary C–Cl bond scission is indicated. Conversion of CCl_2F_2 per flash (f) was as high as 13%; radiant energy absorbed (E_{abs}) was as high as 107 kJ/mol. The plot of $\ln f$ vs. E_{abs}^{-1} is linear with a slope of −419 kJ/mol, which is in good agreement with $-E_{act}$ for thermal decomposition of CCl_2F_2. When CCl_2F_2 is excited at 921 cm^{-1} in the presence of CBr_2F_2 (which does not absorb at 921 cm^{-1}), the absence of organic bromochlorides from the reaction products suggests that reaction takes place in two stages: CCl_2F_2 decomposes very quickly after excitation from a nonequilibrium molecular energy distribution, while CBr_2F_2 reacts thermally after V–T/R relaxation of the absorbed energy.

One of the hopes of infrared laser chemists is that excitation of different vibrational modes will lead to specifically different reactions. A good substrate with which to test this concept is CCl_2F_2, for which the following evidence leads to the expectation of two competing reaction channels: The laser-induced decomposition of the trifluoro analogue, $CClF_3$, involves a free-radical mechanism, while that of CCl_3F involves a carbene mechanism.[2] The corresponding primary processes for CCl_2F_2 are[3]

$$CCl_2F_2 \rightarrow \cdot CClF_2 + Cl\cdot \qquad \Delta H^\circ = 350 \text{ kJ} \qquad (1)$$

$$CCl_2F_2 \rightarrow CF_2 + Cl_2 \qquad \Delta H^\circ = 310 \text{ kJ} \qquad (2)$$

Reactions 1 and 2 are readily distinguished by the nature of the overall reaction products. In the case of (1) one would expect to find ClF_2CCClF_2 and other free-radical products, such as $CClF_3$, while in the case of (2) one would expect to find C_2F_4.

CCl_2F_2 has two strong absorption bands in the CO_2 laser's tunable range.[4,5] The band centered at 923 cm^{-1}, of b_2 symmetry, is formally an antisymmetric CCl_2 stretching mode; the band centered at 1098 cm^{-1}, of a_1 symmetry, is formally a symmetric CF_2 stretching mode. Ngai and Mann[5] describe the dominant normal-coordinate displacements as follows: For the 923-cm^{-1} band, C–Cl stretching, 50%; FCCl bending, 26%. For the 1098-cm^{-1} band, C–F stretching, 59%; C–Cl stretching, 13%.

The thermal decomposition of CCl_2F_2 has been studied at 1 atm between 700 and 900 K.[6] The products are those characteristic of a free-radical mechanism initiated by reaction 1: $CClF_3$, CCl_3F, and the products of their decomposition. ClF_2CCClF_2 is unstable under these conditions. There is also an unidentified white powder formed.

The ultraviolet photolysis of CCl_2F_2[7,8] produces decomposition by both mechanisms 1 and 2. Rebbert and Ausloos[7] find that at 213.9 nm, about 91% of the decomposition occurs